Theoretical framework for stochastic modeling of FxLMS-based active noise control dynamics

Iman Tabatabaei Ardekani, Waleed H. Abdulla
The University of Auckland, New Zealand

***Abstract*—There have been several contributions on theoretical modeling of FxLMS-based active noise control systems; however, when it is intended to derive elegant closed-form expressions for formulating dynamical behaviors of these systems, a number of simplifying assumptions regarding the acoustic noise, the actual secondary path and its model have to be used. This paper develops a dynamic model for FxLMS-based ANC systems, considering a general stochastic acoustic noise and a general secondary path. Also, an arbitrary secondary path model, which is not necessarily a perfect model, is considered. The main distinction of this model is that previously-derived dynamic models can be resulted in from it as special cases.**

I. Introduction

Several mathematical models for the dynamics of the FxLMS-based Active Noise Control (ANC) have been proposed so far [1]–[10]; however, only a few have intended to find closed-form mathematical expressions to model this process. Even if such expressions were derived, simplified cases had to be considered. This is mainly because of the mathematical complexity associated with the modeling of the FxLMS adaptation process. Long summarized early work on this subject in [3], while deriving closed-form expressions for the stability bound (μ_{max}) and steady state performance (J_{ss}) of this process. However, the derivation was based on pure delay secondary paths assumptions. In [5], Elliott derived another expression for μ_{max}, which has become more popular than Long's expression. In [6], Bjarnason conducted a comprehensive analysis of the FxLMS adaptation process. However, once he intended to derive closed-form expressions for μ_{max} and J_{ss}, he had to simplify his formulations by assuming a pure delay secondary path, a perfectly accurate secondary path model, and a broad-band input signal. Also, Vicente derived another expression for μ_{max} when the acoustic noise is assumed to be sum of deterministic sinusoids [11]. All the aforementioned closed-form expressions for μ_{max} were derived for a pure delay secondary path, a perfectly accurate secondary path model and a broad-band input signal. These assumption are not very realistic in many applications of the FxLMS algorithm. Also, practical results show that a reliable μ_{max} is different with those have been proposed in available literature so far [12]. Xiao tried to compute μ_{max} for a realistic secondary path but, as he reported in [13], his theoretical results were not in a good agreement with the simulation results. The authors have investigated behaviors of the FxLMS adaptation process in relatively general and realistic conditions. This investigation has led to a set of closed-form mathematical expressions for formulating behaviors of the FxLMS adaptation process. The results have been published in a series of research papers [7]–[10]. In [7], basic closed-form expressions for formulating behaviors of the FxLMS adaptation process with a general secondary path were derived. In [8], these expressions were generalized by considering the effects of the input signal band-width. Also, in [10] these expressions were generalized further by taking the influences of the imperfect secondary path models into account. The relative drawback of the analysis conducted in [8] is that it is simplified by assuming a perfect secondary path model. Also, the relative drawback of the analysis conducted in [7] is that it is simplified by assuming a broad-band input signal. In fact, the most general case, in which all the available simplifying assumptions are removed, have not been reported yet.

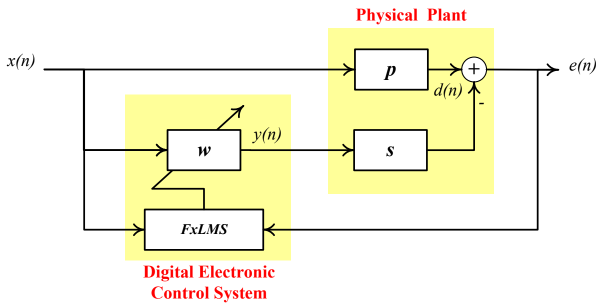

Figure 1: Functional block diagram of FxLMS-based ANC

This paper intends to develop a theoretical framework for stochastic modeling of FxLMS-based ANC dynamics based on the unification of the different models which have previously been developed by the authors. The model developed in this paper is valid for a general case because it is obtained without using any simplifying assumption regarding the secondary path, its model and the acoustic noise bandwidth. The natural extension of this paper will be the derivation of general closed form expressions for the system behaviors. This extension is left to the future work; however, this paper develops the theoretical framework for this.

II. Single Channel Feed-forward ANC

The general block diagram of FxLMS-based ANC is shown in Figure 1. In this figure, $d(n)$ is the noise signal at the desired silence zone, $x(n)$ is the reference signal, measured by the reference microphone, $y(n)$ is the anti-noise signal, generated by the ANC controller, and $e(n)$ is the residual acoustic noise, measured by the error microphone in the silence zone. Also, the primary and secondary paths are shown by linear systems p and s, respectively. According to Figure 1, $d\left(n\right)$ is assumed to be the response of the primary path p to the measured reference signal $x\left(n\right)$. The acoustic signal $d\left(n\right)$ is combined with the anti-noise signal at the desired silence zone. As shown, the anti-noise signal is the actual response of the secondary path s to the control signal $y\left(n\right)$. A realistic secondary path can be represented by a Finite Impulse Response (FIR) system of length Q with an unknown impulse response in the form of

$$s\left(n\right)=\sum_{q=0}^{Q-1}s_q\delta\left(n-q\right) \tag{1}$$

where $\delta\left(n\right)$ is Kronecker delta function and s_q is the amplitude of the impulse response at time index q. Alternatively, this impulse response can be represented in the vector form of

$$\mathbf{s}\triangleq\left[\begin{array}{cccc} s_0 & s_1 & \ldots & s_{Q-1}\end{array}\right]^T \tag{2}$$

The realization of the FxLMS algorithm requires an estimate of the secondary path to be uploaded into the electronic control system. This estimate model, which is usually referred to as the *secondary path model*, can be obtained by using off-line secondary path identification techniques prior to the operation of the ANC system [14], or by using on-line techniques during the operation of the ANC system. Since the actual secondary path is a FIR system, the secondary path model can be assumed to be another FIR system with the impulse response given by

$$\hat{s}\left(n\right)=\sum_{m=0}^{M-1}\hat{s}_m\delta\left(n-m\right) \tag{3}$$

where M is the length of the impulse response ($M<Q$) and scalar parameter $\hat{s}_m$ is the amplitude of the impulse response at time index m. Similar to the actual secondary path impulse response, $\hat{s}\left(n\right)$ can be represented by

$$\hat{\mathbf{s}}\triangleq\left[\begin{array}{cccccc} \hat{s}_0 & \hat{s}_1 & \ldots & \hat{s}_{M-1} & 0 & \ldots & 0\end{array}\right]^T \tag{4}$$

The control signal is generated by an ANC controller w which has a transversal digital filter structure. This digital structure can be adjusted adaptively by using an adaptation algorithm (such as the FxLMS algorithm). Assuming that the ANC controller w has a transversal structure of length L, the control signal $y\left(n\right)$, can be expressed as

$$y\left(n\right)=\mathbf{w}^T\left(n\right)\mathbf{x}\left(n\right) \tag{5}$$

where $\mathbf{x}\left(n\right)$, called the *tap reference vector*, is given by

$$\mathbf{x}\left(n\right)=\left[\begin{array}{cccc} x\left(n\right) & x\left(n-1\right) & \ldots & x\left(n-L+1\right)\end{array}\right]^T \tag{6}$$

and $\mathbf{w}\left(n\right)$, called the (adaptive) *weight vector*, is formed by filter parameters w_0, w_1, ...and w_{L-1} as

$$\mathbf{w}\left(n\right)=\left[\begin{array}{cccc} w_0\left(n\right) & w_1\left(n\right) & \ldots & w_{L-1}\left(n\right)\end{array}\right]^T \tag{7}$$

The FxLMS algorithm performs an adaptation process on $\mathbf{w}\left(n\right)$ in such a way that $y\left(n\right)$ causes the power of $e\left(n\right)$ to be minimized. This algorithm is derived in the following.

Usually, the derivation of the FxLMS algorithm begins with developing a mathematical expression for the residual acoustic noise $e\left(n\right)$. This expression is then optimized with respect to $\mathbf{w}\left(n\right)$. For this purpose, by using Figure 1, $e\left(n\right)$ is initially expressed as

$$e\left(n\right)=d\left(n\right)-\sum_{q=0}^{Q-1}s_q\mathbf{w}^T\left(n-q\right)\mathbf{x}\left(n-q\right) \tag{8}$$

Here, the cost function $J\left(n\right)$ is defined as the power (or variance) of $e\left(n\right)$:

$$J(n)\triangleq E\left\{e^2\left(n\right)\right\} \tag{9}$$

where $E\left\{.\right\}$ denotes the *statistical expectation* operator. This cost function is usually referred to as the *Mean Square Error* (MSE) function. The *optimal weight vector* of an ANC controller, denoted by $\mathbf{w}_o\left(n\right)$, is the weight vector for which the MSE function is minimized. It can be shown that, for a stationary acoustic noise, the optimal weight vector is time-invariant [15]: $\forall n, \mathbf{w}_o\left(n\right)=\mathbf{w}_o$. Accordingly, the optimal residual acoustic noise, denoted by $e_o\left(n\right)$, can be expressed by setting $\mathbf{w}\left(n\right)=\mathbf{w}_o$ in Eq. (8) as

$$e_o\left(n\right)=d\left(n\right)-\mathbf{w}_o^T\mathbf{f}\left(n\right) \tag{10}$$

where $\mathbf{f}\left(n\right)$ is defined as

$$\mathbf{f}\left(n\right)\triangleq\sum_{q=0}^{Q-1}s_q\mathbf{x}\left(n-q\right) \tag{11}$$

Finally, the *minimal MSE*, denoted by J_o, can be obtained by setting $e\left(n\right)=e_o\left(n\right)$ in Eq. (9) as

$$J_o=\sigma_d^2-2\mathbf{w}_o^T\mathbf{p}_f+\mathbf{w}_o^T\mathbf{R}_f\mathbf{w}_o \tag{12}$$

where $\sigma_d^2=E\left\{d^2\left(n\right)\right\}$ is the power of the primary acoustic noise $d\left(n\right)$, $\mathbf{p}_f\triangleq E\left\{\mathbf{f}(n)d(n)\right\}$ is the cross-correlation vector and $\mathbf{R}_f\triangleq E\left\{\mathbf{f}(n)\mathbf{f}^T(n)\right\}$ is the auto-correlation matrix. For a stationary acoustic noise, where $\mathbf{p}_f$ and $\mathbf{R}_f$ are constants, the minimal MSE is time-invariant, and, therefore, it can be represented by J_o. Also, since $\mathbf{w}_o$ minimizes J_o, it can be shown that

$$\mathbf{w}_o=\mathbf{R}_f^{-1}\mathbf{p}_f \tag{13}$$

Finally, combining Eqs. (12) and (13), the optimal MSE is obtained as

$$J_o=\sigma_d^2-\mathbf{p}_f^T\mathbf{R}_f^{-1}\mathbf{p}_f \tag{14}$$

In signal processing, the optimal weight vector, given in Eq. (13), is usually referred to as the *Wiener-Hopf optimal filter*. Also, the value of J_o is referred to as the minimum achievable MSE function. In ANC literature, J_o can be interpreted as the minimum achievable residual acoustic noise power. Note that J_o is only a function of acoustic noise statistics and impulse responses of primary and secondary paths. In other words, J_o is independent of instantaneous values of the acoustic noise and operational parameters of the FxLMS algorithms (e.g. step-size and secondary path model).

The optimal weight vector, given in Eq. (13), can be directly calculated from $\mathbf{R}_f$ and $\mathbf{p}_f$; however, estimation of $\mathbf{R}_f$ and $\mathbf{p}_f$ requires a considerable amount of computation. Another approach to determining the optimal weight vector is based on using the *steepest-descent method* [16]. According to this method, if the weight vector $\mathbf{w}(n)$ is updated by the following equation, then it is bound to move towards the optimal solution given in Eq. (13).

$$\mathbf{w}(n+1) = \mathbf{w}(n) - \frac{1}{2}\mu\nabla J(n) \quad (15)$$

It can be shown that [14]

$$\nabla J(n) = -2e(n)\,\mathbf{f}(n) \quad (16)$$

Now, the FxLMS update equation can be obtained by substituting Eq. (16) into (15) as

$$\mathbf{w}(n+1) = \mathbf{w}(n) + \mu e(n)\,\mathbf{f}(n) \quad (17)$$

In practice, $\mathbf{f}(n)$ is not physically available, therefore, the implementation of Eq. (17) requires an estimate of $\mathbf{f}(n)$. This estimate can be obtained by filtering $\mathbf{x}(n)$ using the available estimate of the secondary path, given in Eq. (3). Therefore, the estimate of $\mathbf{f}(n)$, denoted by $\hat{\mathbf{f}}(n)$, can be obtained by

$$\hat{\mathbf{f}}(n) = \sum_{m=0}^{M-1} \hat{s}_m \mathbf{x}(n-m) \quad (18)$$

Usually, $\hat{\mathbf{f}}(n)$ is called the *filtered reference vector*. Now, by replacing $\mathbf{f}(n)$ with $\hat{\mathbf{f}}(n)$ in Eq. (16), $\nabla J(n)$ is approximated by

$$\nabla J(n) \approx -2e(n)\,\hat{\mathbf{f}}(n) \quad (19)$$

Also, the updating equation, given in Eq. (15), becomes

$$\mathbf{w}(n+1) = \mathbf{w}(n) + \mu e(n)\,\hat{\mathbf{f}}(n) \quad (20)$$

Eq. (20) can be implemented using available signals and parameters. $\hat{\mathbf{f}}(n)$ can be obtained by filtering the reference signal and buffering the obtained values as

$$\hat{\mathbf{f}}(n) = \left[\begin{array}{cccc} \hat{f}(n) & \hat{f}(n-1) & \ldots & \hat{f}(n-L+1) \end{array}\right]^T \quad (21)$$

where $\hat{f}(n)$ is the *filtered-reference signal* given by

$$\hat{f}(n) = \sum_{m=0}^{M-1} \hat{s}_m x(n-m) \quad (22)$$

Eqs. (20)-(22) give a formulation for the FxLMS algorithm, which can be implemented practically.

A. Rotated Vectors

In the analysis of a gradient-based adaptation algorithm, it is more convenient to use the rotated reference vector and rotated weight misalignment vector, instead of the original reference and weight vectors [16]. This is because the auto-correlation matrix of the rotated reference vector is diagonal, and the equilibrium point of the rotated weight misalignment vector is the origin, rather than the Wiener-Hopf solution. In the following, these rotated vectors are introduced. The *Auto-Correlation Matrix* (ACM) of the reference vector is defined as

$$\mathbf{R} \triangleq E\left\{\mathbf{x}(n)\,\mathbf{x}^T(n)\right\} \quad (23)$$

Since $\mathbf{R}$ is a Toeplitz matrix, it can be diagonalized as

$$\mathbf{R} = \mathbf{F}\boldsymbol{\Lambda}\mathbf{F}^T \quad (24)$$

where square matrix $\mathbf{F}$ is the modal matrix, formed by the Eigenvectors $\mathbf{F}_0$, $\mathbf{F}_1$,... , $\mathbf{F}_{L-1}$ and diagonal matrix $\boldsymbol{\Lambda}$ is formed by the Eigenvalues λ_0, λ_1, ... ,λ_{L-1}:

$$\boldsymbol{\Lambda} = diag\left(\lambda_0, \lambda_1, \ldots, \lambda_{L-1}\right) \quad (25)$$

The inverse of any modal matrix is equal to its transpose; thus: $\mathbf{F}^T\mathbf{F} = \mathbf{I}$. In this case, it can be shown that

$$\mathbf{F}^T\mathbf{R}\mathbf{F} = \boldsymbol{\Lambda} \quad (26)$$

Using the modal matrix $\mathbf{F}$ as a rotation matrix, the *rotated reference vector* is defined as:

$$\mathbf{z}(n) \triangleq \mathbf{F}^T\mathbf{x}(n) \quad (27)$$

This vector can be expressed in the form of

$$\mathbf{z}(n) = \left[\begin{array}{cccc} z_0(n) & z_1(n) & \ldots & z_{L-1}(n) \end{array}\right]^T \quad (28)$$

From Eq. (27), it can be shown that the l-th element of $\mathbf{z}(n)$ can be computed as

$$z_l(n) = \mathbf{F}_l^T\mathbf{x}(n), \qquad l = 0, 1, \ldots, L-1 \quad (29)$$

where vector $\mathbf{F}_l$ is the l-th column of matrix $\mathbf{F}$. The rotated weight misalignment vector is defined as

$$\mathbf{c}(n) \triangleq \mathbf{F}^T\left(\mathbf{w}(n) - \mathbf{w}_o\right). \quad (30)$$

This vector can be also represented in the form of

$$\mathbf{c}(n) = \left[\begin{array}{cccc} c_0(n) & c_1(n) & \ldots & c_{L-1}(n) \end{array}\right]^T. \quad (31)$$

where $c_l(n)$ is computed as

$$c_l(n) = \mathbf{F}_l^T\left(\mathbf{w}(n) - \mathbf{w}_o\right),, \qquad l = 0, 1, \ldots, L-1. \quad (32)$$

As can be seen in Eq. (32), when $\mathbf{w}(n)$ converges to $\mathbf{w}_o$, the rotated weight misalignment vector converges to the origin. Due to this property, the analysis of the FxLMS algorithm using the rotated weight misalignment vector is more convenient.

Now, In order to express the FxLMS update equation in terms of the rotated variables, Eq. (20) must be added by $-\mathbf{w}_o$ and then left multiplied by $\mathbf{F}^T$. In this case, it can be shown that

$$\mathbf{c}(n+1) = \mathbf{c}(n) + \mu e(n)\mathbf{F}^{\mathbf{T}}\hat{\mathbf{f}}(n) \quad (33)$$

Now, the rotated filtered reference vector is defined as

$$\hat{\mathbf{g}}(n) = \mathbf{F}^{\mathbf{T}}\hat{\mathbf{f}}(n) \quad (34)$$

By using this definition, Eq. (33) can be re-expressed as

$$\mathbf{c}(n+1) = \mathbf{c}(n) + \mu e(n)\hat{\mathbf{g}}(n) \quad (35)$$

According to Eqs. (18), (27) and (34), vector $\hat{\mathbf{g}}(n)$ can be obtained by filtering $\mathbf{z}(n)$ using the available estimate of the secondary path:

$$\hat{\mathbf{g}}(n) = \sum_{m=0}^{M-1} \hat{s}_m \mathbf{z}(n-m) \quad (36)$$

Alternatively, $\hat{\mathbf{g}}(n)$ can be also represented in the form of

$$\hat{\mathbf{g}}(n) = \begin{bmatrix} \hat{g}_0(n) & \hat{g}_1(n) & \ldots & \hat{g}_{L-1}(n) \end{bmatrix}^T \tag{37}$$

$$\hat{g}_l(n) = \sum_{m=0}^{M-1} \hat{s}_m z_l(n-m) \tag{38}$$

Eqs. (35)-(38) describe the FxLMS update equation in terms of the rotated variables. Using the same logic, Eq. (8) can be expressed in terms of the rotated variables as [8]

$$e(n) = e_o(n) - \sum_{q=0}^{Q-1} s_q \mathbf{z}^T(n-q)\,\mathbf{c}(n-q) \tag{39}$$

B. Independence Assumptions

The analysis of gradient-based adaptation algorithms with stochastic reference signals is usually performed based on a set of simplifying assumptions, called the *independence assumptions*. These assumptions were proposed by Gardener in a signal processing context [17]; however, they have been widely used in analyzing adaptive ANC systems. As Gardener stated in [17], "the independence assumptions apparently cannot be analytically justified for practical cases, but this is perhaps the best that can be done from the pragmatic point of view of obtaining a good trade-off between model realism and model tractability". In the following, these assumptions are discussed and formulated in detail. Later, the validity of the theoretical results obtained by using these assumptions are verified in computer simulation and practice.

The primary independence assumption: this assumption states that, for a Gaussian reference signal, the sequence of reference vectors can be considered as an *independent identically distributed* (i.i.d) sequence with zero mean [17]. Accordingly, consecutive reference vectors are statistically independent. Based on this assumption, it can be shown that

$$E\left\{\mathbf{x}(n-m)\,\mathbf{x}^T(n-p)\right\} = \delta_{m,p}\mathbf{R} \qquad \forall n,m,p \in \mathbb{N} \tag{40}$$

Also, by using Eqs. (27) and (40), it can be shown that

$$E\left\{\mathbf{z}(n-m)\,\mathbf{z}^T(n-p)\right\} = \delta_{m,p}\mathbf{\Lambda} \qquad \forall n,m,p \in \mathbb{N}, \tag{41}$$

The secondary independence assumption: according to this assumption, for the problem of adaptive identification of an unknown system with finite impulse response, the optimal error $e_o(n)$ is independent of both the reference and rotated reference vectors. [17]. Since the reference vector has zero mean, the following results can be obtained

$$E\left\{e_o(n_1)\,\mathbf{x}(n_2)\right\} = \mathbf{0} \tag{42}$$

and

$$E\left\{e_o(n_1)\,\mathbf{z}(n_2)\right\} = \mathbf{0} \tag{43}$$

Therefore, the optimal residual acoustic noise is uncorrelated with both the reference and rotated reference vectors.

The third independence assumption: Usually it is assumed that the weights of the ANC controller and samples of the reference signal are statistically independent [15], [18]. Based on this assumption, it can be shown that

$$E\left\{\mathbf{w}^T(n_1)\,\mathbf{x}(n_2)\right\} = E\left\{\mathbf{w}^T(n_1)\right\}E\left\{\mathbf{x}(n_2)\right\} \tag{44}$$

Also, from this equality, it can be shown that $\mathbf{c}(n)$ and $\mathbf{z}(n)$ are statistically independent

$$E\left\{\mathbf{c}^T(n_1)\,\mathbf{z}(n_2)\right\} = E\left\{\mathbf{c}^T(n_1)\right\}E\left\{\mathbf{z}(n_2)\right\} \tag{45}$$

III. Development of a Dynamic Model for the FxLMS-based ANC

This section derives a dynamic model for the FxLMS-based ANC. For this purpose, the MSE function is initially expressed by combining Eqs. (9) and (39) as

$$J(n) = E\left\{e_o^2(n)\right\} - 2\sum_{q=0}^{Q-1} s_q E\left\{\mathbf{c}^T(n-q)\,\mathbf{z}(n-q)\,e_o(n)\right\} + \sum_{q,p=0}^{Q-1} s_q s_p E\left\{\mathbf{c}^T(n-q)\,\mathbf{z}(n-q)\,\mathbf{z}^T(n-p)\,\mathbf{c}(n-p)\right\} \tag{46}$$

The first term in Eq. (46) is equal to J_o. The second term is equal to zero because based on the independence assumptions, the rotated reference vector $\mathbf{z}(n-q)$ is a zero mean vector and statistically independent of $e_o(n)$ and $\mathbf{c}(n)$. Therefore, Eq. (46) can be simplified to

$$J(n) = J_o + \sum_{q,p=0}^{Q-1} s_q s_p E\left\{\mathbf{c}^T(n-q)\,\mathbf{z}(n-q)\,\mathbf{z}^{\mathbf{T}}(n-p)\,\mathbf{c}(n-p)\right\} \tag{47}$$

Now, combining Eqs. (28), (31) and (47) results in

$$J(n) = J_o + \sum_{q,p=0}^{Q-1}\sum_{l,k=0}^{L-1} s_q s_p E\left\{c_l(n-q)\,c_k(n-p)\,z_l(n-q)\,z_k(n-p)\right\} \tag{48}$$

Using the third independence assumption, Eq. (48) can be simplified to

$$J(n) = J_o + \sum_{q,p=0}^{Q-1}\sum_{l,k=0}^{L-1} s_q s_p E\left\{z_l(n-q)\,z_k(n-p)\right\} \times E\left\{c_l(n-q)\,c_k(n-p)\right\} \tag{49}$$

Combining Eqs. (29) and (49) results in

$$J(n) = J_o + \sum_{q,p=0}^{Q-1}\sum_{l,k=0}^{L-1} s_q s_p \mathbf{F}_l^T E\left\{\mathbf{x}(n-q)\,\mathbf{x}^T(n-p)\right\} \times \mathbf{F}_k E\left\{c_l(n-q)\,c_k(n-p)\right\} \tag{50}$$

Now, combining Eqs. (40) and (50) results in

$$J(n) = J_o + \sum_{q=0}^{Q-1}\sum_{l,k=0}^{L-1} s_q^2 \mathbf{F}_l^T \mathbf{R} \mathbf{F}_k E\left\{c_l(n-q)\,c_k(n-q)\right\} \tag{51}$$

On the other hand, from Eq. (26), it can be shown that

$$\mathbf{F}_l^T \mathbf{R} \mathbf{F}_k = \lambda_l \delta_{l,k} \tag{52}$$

Using this equality, Eq. (51) is simplified to

$$J(n) = J_o + \sum_{q=0}^{Q-1} \sum_{l=0}^{L-1} s_q^2 \lambda_l E\left\{c_l^2(n-q)\right\} \tag{53}$$

Finally, Eq. (53) can be expressed in the form of

$$J(n) = J_o + \sum_{q=0}^{Q-1} s_q^2 E\left\{\mathbf{c}^T(n-q)\,\mathbf{\Lambda}\mathbf{c}(n-q)\right\} \tag{54}$$

From Eq. (54), it can be seen that $J(n)$ is independent of instantaneous values of the acoustic noise. Also, it can be deduced that $J(n)$ is a positive scalar function of $\mathbf{c}(n)$.

A. Excess-MSE Function

Here, the *excess-MSE function* is defined as a dynamic measure, determining the deviation of the MSE function from its minimal level. Usually, the steady-state level of this function is referred to as the excess-MSE in ANC terminology. However, the excess-MSE function, which can be interpreted as the distance of the instantaneous residual noise power from the minimum achievable noise power, is considered in this thesis. Accordingly, dynamics of an ANC system can be studied by analyzing the variation of the excess-MSE function during the operation of the adaptation algorithm on the ANC controller. For developing a dynamic model for the excess-MSE function, the MSE function is expressed as

$$J(n) = J_o + J_{ex}(n) \tag{55}$$

where J_o is the minimal MSE level and $J_{ex}(n)$ is the excess-MSE function. As can be seen in Eq. (55), the absolute value of $J_{ex}(n)$ determines how far the instantaneous residual noise power is from its minimal level. Obviously, since J_o is the minimal value of the positive definite function $J(n)$, $J_{ex}(n)$ is always a positive definite function of system variables:

$$J_{ex}(n) \geq 0 \tag{56}$$

Now, considering the expressions, given in Eqs. (54) and (55), $J_{ex}(n)$ can be formulated as

$$J_{ex}(n) \triangleq \sum_{q=0}^{Q-1} s_q^2 E\left\{\mathbf{c}^T(n-q)\,\mathbf{\Lambda}\mathbf{c}(n-q)\right\} \tag{57}$$

Substituting

$$J_{ex}(n) = \sum_{q=0}^{Q-1} \sum_{l=0}^{L-1} \lambda_l s_q^2 m_l(n-q) \tag{58}$$

where $m_0(n), m_1(n), \ldots, m_{L-1}(n)$ are the *second-order moments of the adaptive weights*:

$$m_l(n) \triangleq E\left\{c_l^2(n)\right\} \qquad l = 0, 1, \ldots, L-1 \tag{59}$$

Now, in order to investigate the variation of the excess-MSE function during the operation of the FxLMS algorithm, its time difference is defined as

$$\triangle J_{ex}(n) \triangleq J_{ex}(n+1) - J_{ex}(n) \tag{60}$$

By combining Eqs. (58) and (60), $\triangle J_{ex}(n)$ can be expressed as

$$\triangle J_{ex}(n) = \sum_{q=0}^{Q-1} \sum_{l=0}^{L-1} \lambda_l s_q^2 \triangle m_l(n-q) \tag{61}$$

where $\triangle m_l(n)$ is the time difference of the l-th second-order moment. From Eq. (59), $\triangle m_l(n)$ can be expressed as

$$\triangle m_l(n) = E\left\{c_l^2(n+1)\right\} - E\left\{c_l^2(n)\right\} \tag{62}$$

On the other hand, from Eq. (35), it can be shown that

$$c_l(n+1) = c_l(n) + \mu \hat{g}_l(n)\, e(n) \tag{63}$$

By combining Eqs. (62) and (63), $\triangle m_l(n)$ is formulated by

$$\triangle m_l(n) = \mu^2 E\left\{\hat{g}_l^2(n)\, e^2(n)\right\} + 2\mu E\left\{c_l(n)\,\hat{g}_l(n)\, e(n)\right\} \tag{64}$$

On the other hand, from Eqs. (18), (29) and (38), it can be shown that

$$\hat{g}_l(n) = \mathbf{F}_l^T \hat{\mathbf{f}}(n) \tag{65}$$

By substituting the above expression for $\hat{g}_l(n)$ into Eq. (64), $\triangle m_l(n)$ is obtained as

$$\triangle m_l(n) = A_l(n) + B_l(n) \tag{66}$$

where scalar functions $A_l(n)$ and $B_l(n)$ are given by

$$A_l(n) = \mu^2 \mathbf{F}_l^T E\left\{\hat{\mathbf{f}}(n)\, \hat{\mathbf{f}}^T(n)\, e^2(n)\right\} \mathbf{F}_l \tag{67}$$

and

$$B_l(n) = 2\mu \mathbf{F}_l^T E\left\{\hat{\mathbf{f}}(n)\, c_l(n)\, e(n)\right\} \tag{68}$$

The mathematical expressions, given in Eqs. (61) and (66)-(68), compose a stochastic dynamic model for the variation of the excess-MSE function during the operation of the FxLMS algorithm. The following two sections formulate scalar functions $A_l(n)$ and $B_l(n)$.

Variation of $A_l(n)$:

Based on the third independence assumption, it can be shown that the reference vector $\mathbf{x}(n)$ is independent of the MSE function $J(n)$ [19]. Consequently, the filtered reference vector $\hat{\mathbf{f}}(n)$ is independent of $J(n)$. Accordingly, Eq. (67) can be simplified to

$$A_l(n) = \mu^2 \mathbf{F}_l^T E\left\{\hat{\mathbf{f}}(n)\, \hat{\mathbf{f}}^T(n)\right\} \mathbf{F}_l . J(n) \tag{69}$$

On the other hand, from Eqs. (18) and (40) , it can be shown that

$$E\left\{\hat{\mathbf{f}}(n)\, \hat{\mathbf{f}}^T(n)\right\} = \|\hat{\mathbf{s}}\|^2 \mathbf{R} \tag{70}$$

where $\|.\|$ denotes the Euclidean vector norm and vector $\hat{\mathbf{s}}$ is given in Eq. (4). Now, by substituting Eq. (70) into (69), $A_l(n)$ is simplified to

$$A_l(n) = \mu^2 \|\hat{\mathbf{s}}\|^2 \mathbf{F}_l^T \mathbf{R} \mathbf{F}_l J(n) \tag{71}$$

From Eq. (26) , it can be shown that $\mathbf{F}_l^T \mathbf{R} \mathbf{F}_l = \lambda_l$; substituting this equality into Eq. (71) results in

$$A_l(n) = \mu^2 \lambda_l \|\hat{\mathbf{s}}\|^2 J(n) \tag{72}$$

Now, substituting Eq. (55) into Eq. (72) results in

$$A_l(n) = \mu^2 \lambda_l \|\hat{\mathbf{s}}\|^2 J_o + \mu^2 \lambda_l \|\hat{\mathbf{s}}\|^2 J_{ex}(n) \tag{73}$$

Finally, by using Eq. (58), Eq (73) can be expressed as

$$A_l(n) = \mu^2 \lambda_l \|\hat{\mathbf{s}}\|^2 J_o + \mu^2 \lambda_l \|\hat{\mathbf{s}}\|^2 \sum_{p=0}^{Q-1} \sum_{k=0}^{L-1} \lambda_k s_p^2 m_k(n-p) \tag{74}$$

Eq. (74) formulates $A_l(n)$ as a function of the second-order moments $m_o(n), \ldots, m_{L-1}(n)$.

Variation of $B_l(n)$:

By substituting Eq. (39) into (68), $B_l(n)$ is expanded to

$$B_l(n) = 2\mu \mathbf{F}_l^T E\left\{\hat{\mathbf{f}}(n) c_l(n) e_o(n)\right\}$$
$$-2\mu \mathbf{F}_l^T \sum_{p=0}^{Q-1} s_p E\left\{c_l(n) \hat{\mathbf{f}}(n) \mathbf{c}^T(n-p) \mathbf{z}(n-p)\right\} \tag{75}$$

Considering the second and third independence assumptions, the first term in Eq. (75) is simplified to $2\mu \mathbf{F}_l^T E\left\{\hat{\mathbf{f}}(n)\right\} E\{c_l(n) e_o(n)\}$. Since the reference signal has zero mean, it can be shown that $E\{\hat{\mathbf{f}}(n)\} = \mathbf{0}$; therefore, $2\mu \mathbf{F}_l^T E\left\{\hat{\mathbf{f}}(n) c_l(n) e_o(n)\right\} = 0$. Using this result, $B_l(n)$ is simplified to

$$B_l(n) = -2\mu \mathbf{F}_l^T \sum_{p=0}^{Q-1} s_p E\left\{c_l(n) \hat{\mathbf{f}}(n) \mathbf{c}^T(n-p) \mathbf{z}(n-p)\right\} \tag{76}$$

Now, using Eqs. (18), (28), (31) and (76) results in

$$B_l(n) = -2\mu \mathbf{F}_l^T \sum_{p=0}^{Q-1} \sum_{m=0}^{M-1} \sum_{i=0}^{L-1} s_p \hat{s}_m \times \tag{77}$$
$$E\{c_l(n) c_i(n-p) \mathbf{x}(n-m) z_i(n-p)\}$$

On the other hand, from Eq. (29), it can be shown that

$$z_i(n-p) = \mathbf{x}^T(n-p) \mathbf{F}_i \tag{78}$$

Combining Eqs. (77) and (78) and the third independence assumption, Eq. (77) can be simplified to

$$B_l(n) = -2\mu \mathbf{F}_l^T \sum_{p=0}^{Q-1} \sum_{m=0}^{M-1} \sum_{i=0}^{L-1} s_p \hat{s}_m E\{c_l(n) c_i(n-p)\} \times \tag{79}$$
$$E\left\{\mathbf{x}(n-m) \mathbf{x}^T(n-p)\right\} \mathbf{F}_i$$

Now, substituting Eq. (40) into (79) results in

$$B_l(n) = -2\mu \sum_{p=0}^{Q-1} \sum_{i=0}^{L-1} s_p \hat{s}_p E\{c_l(n) c_i(n-p)\} \mathbf{F}_l^T \mathbf{R} \mathbf{F}_i \tag{80}$$

Note that, according to Eq. (4), for $m > M-1$, $\hat{s}_m = 0$. On the other hand, Eq. (26) results in $\mathbf{F}_l^T \mathbf{R} \mathbf{F}_i = \lambda_l \delta_{l,i}$. By using this equality, Eq.(80) is simplified to

$$B_l(n) = -2\mu \lambda_l \sum_{p=0}^{Q-1} s_p \hat{s}_p E\{c_l(n) c_l(n-p)\} \tag{81}$$

From the FxLMS update equation, given in Eq. (35), it can be shown that for $p = 0, 1, \ldots, Q-1$

$$\mathbf{c}(n) = \mathbf{c}(n-p) + \mu \sum_{k=1}^{p} \hat{\mathbf{g}}(n-k) e(n-k) \tag{82}$$

When the adaptation process is slow, Eq. (82) can be approximated by

$$\mathbf{c}(n) \approx \mathbf{c}(n-p) + \mu p \hat{\mathbf{g}}(n-p) e(n-p) \tag{83}$$

Therefore, for the variation of the l-th adaptive weight, the following equation can be derived.

$$c_l(n) \approx c_l(n-p) + \mu p \hat{g}_l(n-p) e(n-p) \tag{84}$$

Now, combining Eqs. (81) and (84) results in

$$B_l(n) = -2\mu \lambda_l \sum_{p=0}^{Q-1} s_p \hat{s}_p E\left\{c_l^2(n-p)\right\} \tag{85}$$
$$-2\mu^2 \lambda_l \sum_{p=0}^{Q-1} p s_p \hat{s}_p E\{c_l(n-p) \hat{g}_l(n-p) e(n-p)\}$$

By using Eqs. (59), (65) and (68), Eq. (85) can be expressed as

$$B_l(n) = -2\mu \lambda_l \sum_{p=0}^{Q-1} s_p \hat{s}_p m_l(n-p) - \tag{86}$$
$$\mu \lambda_l \sum_{p=0}^{Q-1} p s_p \hat{s}_p B_l(n-p)$$

By changing the index of the second summation in Eq. (86), $B_l(n)$ can be re-expressed as

$$B_l(n) = -2\mu \lambda_l \sum_{p=0}^{Q-1} s_p \hat{s}_p m_l(n-p) - \tag{87}$$
$$\mu \lambda_l \sum_{r=0}^{Q-1} r s_r \hat{s}_r B_l(n-r)$$

The recursive equation, given in Eq. (87), can be expanded to

$$\begin{aligned} B_l(n) &= -2\mu \lambda_l \sum_{p=0}^{Q-1} s_p \hat{s}_p m_l(n-p) \\ &+ 2\mu^2 \lambda_l^2 \sum_{p=0}^{Q-1} s_p \hat{s}_p \sum_{r=0}^{Q-1} r s_r \hat{s}_r m_l(n-p-r) \\ &\vdots \end{aligned} \tag{88}$$

For $\mu \ll 1$, Eq. (88) is approximated by its two first terms:

$$B_l(n) \approx -2\mu \lambda_l \sum_{p=0}^{Q-1} s_p \hat{s}_p m_l(n-p) + \tag{89}$$
$$2\mu^2 \lambda_l^2 \sum_{p,r=0}^{Q-1} r s_p \hat{s}_p s_r \hat{s}_r m_l(n-p-r)$$

Eq. (89) formulates $B_l(n)$ as a function of the second-order moments $m_o(n), \ldots, m_{L-1}(n)$.

Using the expressions, obtained in Sections 3.3 and 3.4, this section develops an stochastic model for the excess-MSE function. For this purpose, $\triangle m_l(n)$ can be initially expressed by substituting Eqs. (74) and (89) into Eq. (66) . Subsequently, substituting the obtained expression for $\triangle m_l(n)$ into Eq. (61) gives the following expression for $\triangle J_{ex}(n)$.

$$\triangle J_{ex}(n) = \mu^2 \|\hat{\mathbf{s}}\|^2 \|\mathbf{s}\|^2 \lambda_{rms}^2 L J_o \tag{90}$$
$$+\mu^2 \|\hat{\mathbf{s}}\|^2 L\lambda_{rms}^2 \sum_{q,p=0}^{Q-1}\sum_{k=0}^{L-1} \lambda_k s_q^2 s_p^2 m_k(n-p-q)$$
$$-2\mu \sum_{p,q=0}^{Q-1}\sum_{l=0}^{L-1} \lambda_l^2 s_q^2 s_p \hat{s}_p m_l(n-p-q)$$
$$+2\mu^2 \sum_{q,p,r=0}^{Q-1}\sum_{l=0}^{L-1} r\lambda_l^3 s_q^2 s_p \hat{s}_p s_r \hat{s}_r m_l(n-p-r-q)$$

where λ_{rms} is the RMS (Root Mean Square) value of the Eigenvalues" $\lambda_{rms} = \left(\frac{1}{L}\sum_{l=0}^{L-1}\lambda_l^2\right)^{0.5}$. In a slow adaptation process, the second-order moments are updated slowly so that:

$$m_l(n-p-r-q) \approx m_l(n-p-q), \qquad r = 0,1,\ldots,L-1 \tag{91}$$

By using this assumption, Eq. (90) is simplified to

$$\triangle J_{ex}(n) = \mu^2 \|\hat{\mathbf{s}}\|^2 \|\mathbf{s}\|^2 \lambda_{rms}^2 L J_o \tag{92}$$
$$+\mu^2 \|\hat{\mathbf{s}}\|^2 L\lambda_{rms}^2 \sum_{q,p=0}^{Q-1}\sum_{k=0}^{L-1} \lambda_k s_q^2 s_p^2 m_k(n-p-q)$$
$$-2\mu \sum_{q,p=0}^{Q-1}\sum_{l=0}^{L-1} \lambda_l^2 s_q^2 s_p \hat{s}_p m_l(n-p-q)$$
$$+2\mu^2 \left(\sum_{r=0}^{Q-1} r s_r \hat{s}_r\right) \sum_{q,p=0}^{Q-1}\sum_{l=0}^{L-1} \lambda_l^3 s_q^2 s_p \hat{s}_p m_l(n-p-q)$$

Now, by defining diagonal matrix $\mathbf{\Psi}$ as

$$\mathbf{\Psi} = diag(0,1,\ldots,Q-1) \tag{93}$$

it can be shown that

$$\sum_{r=0}^{Q-1} r s_r \hat{s}_r = \mathbf{s}^T \mathbf{\Psi} \hat{\mathbf{s}} \tag{94}$$

Substituting Eq. (94) into (92) results in

$$\triangle J_{ex}(n) = \mu^2 \|\hat{\mathbf{s}}\|^2 \|\mathbf{s}\|^2 \lambda_{rms}^2 L J_o - \tag{95}$$
$$\mu \sum_{q,p=0}^{Q-1}\sum_{l=0}^{L-1} \gamma_{l,p,q} m_l(n-p-q)$$

where scalar parameter $\gamma_{l,p,q}$ is defined as

$$\gamma_{l,p,q} = \lambda_l s_q^2 \Bigg[2\lambda_l s_p \hat{s}_p - \mu\lambda_{rms}^2 \|\hat{\mathbf{s}}\|^2 \Bigg(L s_p^2 \tag{96}$$
$$+2\left(\frac{\lambda_l}{\lambda_{rms}}\right)^2 \times \frac{\mathbf{s}^T\mathbf{\Psi}\hat{\mathbf{s}}}{\|\hat{\mathbf{s}}\|^2} s_p \hat{s}_p \Bigg) \Bigg]$$

Eqs. (60), (95) and (96) describe a linear stochastic model for the excess-MSE function, considering an arbitrary acoustic noise, an arbitrary secondary path, and an arbitrary secondary path model.

IV. Simulation Results

Figure 2 shows the primary and secondary paths impulse responses of the simulated ANC system. Also, Figure 3 shows impulse responses of the two imperfect secondary path models (M_1 and M_2), used in the implementation of the FxLMS algorithm. In this figure, the impulse response of the actual secondary path (perfect model) is also shown by a dashed line. Figure 4 shows the power spectrum of the broad-band white signal, generated by the computer to be used as the reference signal $x(n)$ in simulation experiments. As can be seen, the power spectrum of this signal is approximately flat over its entire frequency range. Hence, this signal can be considered as a broad-band white signal. The total power of the signal is limited to $\sigma_x^2 = 1$. By passing this broad-band signal through standard low-pass filters, different band-limited white signals can be produced. For example, by using a low-pass filter of normalized band-width 0.5, a band-limited reference signal with band-width $B_w = 0.5$ can be produced. The power spectrum of such signal is shown in Figure 4. The magnitude of the obtained signal is scaled in such a way that its power remains constant at $\sigma_x^2 = 1$. Using the same procedure, different band-limited reference signals with different band-widths can be generated.

Note that, in Figures 4, blue solid lines show the power spectrum, obtained using numerical methods and red dashed lines show the theoretical power spectrum, as it is assumed in our theoretical investigations. In addition to this theoretical assumption, the independence assumptions are used in the derivation of the analytical model developed in Chapter 3. Based on this model, most of the theoretical contributions of Chapters 4-6 are obtained. Therefore, before checking the validity of the derived theoretical results, it is necessary to check the general validity of this fundamental model.

A. Dynamic Simulation

Here, it is shown that the model, developed in Chapter 3, can precisely describe behaviors of the simulated FxLMS-based ANC system, despite using theoretical independence assumptions in the derivation of this model. Each simulation experiment includes 100 simulation runs with independent noise sequences (reference signal). The variation of the square of the residual acoustic noise, obtained from each run, is stored in the computer memory. The MSE function is then estimated by averaging over the stored data. Now, it is required to find an estimate for the excess-MSE function form the obtained simulation results. According to Eq. (55), it can be shown that the difference of the excess-MSE function, $\triangle J_{ex}(n)$, is equal to the difference of $\triangle J(n)$; therefore, $\triangle J_{ex}(n)$ can be evaluated as

$$\triangle J_{ex}(n) = J(n+1) - J(n) \tag{97}$$

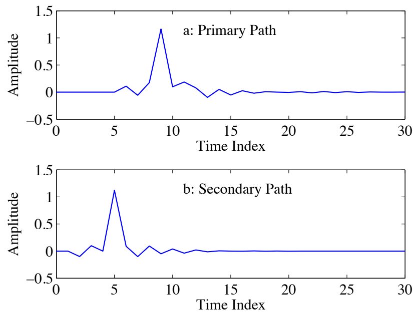

Figure 2: Impulse responses of primary and secondary paths in computer simulation

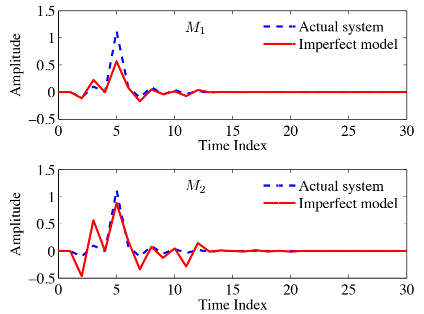

Figure 3: Impulse responses of secondary path models

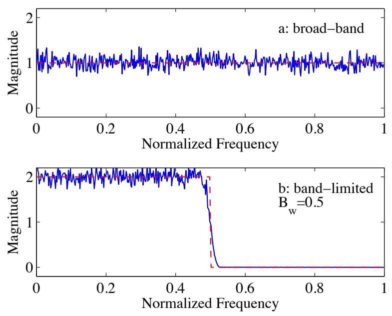

Figure 4: Power spectrum of two reference signals generated by computer ($\sigma_x^2 = 1$)

Now, the variation of $\triangle J_{ex}(n)$ can be computed using the data obtained from the computer simulation. On the other hand, the theoretical variation of $\triangle J_{ex}(n)$ can be computed by using the analytical model, given in Eqs. (95) and (96). Accordingly, comparing the result obtained from this model and the one obtained from the computer simulation leads to the verification of the validity of the proposed theoretical model. For this purpose, several simulation experiments in different cases are conducted.

In the first case, simulation experiments are conducted in classical working conditions, which were usually considered in the theoretical analysis of FxLMS-based ANC systems. In these conditions, the reference signal is assumed to be a broad-band white stochastic signal with a flat power spectrum, as shown in Figure 4a. Also, the secondary path model is assumed to be a perfectly accurate model (identical to the actual secondary path).

In this situation, two simulation experiments with two different step-sizes are conducted. In the first experiment, a relatively small step-size of $\mu = 0.005$ and in the second one a relatively large step-size of $\mu = 0.05$ is used. The variation of $\triangle J_{ex}(n)$ for each experiment can be then plotted, as shown in Figure 5a (blue lies). Also, the theoretical variation of $\triangle J_{ex}(n)$, obtained from Eqs. (95) and (96) is shown in Figure 5a by using red lines. As can be seen, the proposed theoretical model can precisely describe behaviors of the simulated system in both the transient and steady-state modes.

In the second case, band-limited acoustic noise signals are considered; however, the secondary path model is still set to a perfect model. In this situation, two experiments with two different band-limited signals are conducted ($B_w = 0.2$ and $B_w = 0.8$). In both of the experiments, the step-size is set to $\mu = 0.005$. For each experiment, experimental and theoretical variations of $\triangle J_{ex}(n)$ are plotted in Figure 5b. The agreement between the theoretical and simulation results is evident. This agreement can be also shown for other values of the step-size.

In the third case, a broad-band white noise, as described in Case 1, is considered; however, imperfect secondary path models M_1 and M_2, shown in Figure 3, are used in the FxLMS algorithm. For each secondary path model, a separate experiment is conducted. In both of the experiments, the step-size is set to $\mu = 0.005$. Theoretical and experimental variations of $\triangle J_{ex}(n)$ are plotted in Figure 5c. As this figure shows, the proposed theoretical model can precisely describe the simulated system behaviors in both the transient and steady-state modes.

Now, the most general case with a band-limited noise and an imperfect secondary path model is considered. In this case, the acoustic noise is a band-limited white signal of band-width $B_w = 0.8$, and the secondary path model is set to M_1. Two simulation experiments for relatively small step-size of $\mu = 0.005$ and relatively large step-size of $\mu = 0.05$ are conducted. The variation of $\triangle J_{ex}(n)$ for each experiment is plotted in Figure 5d. Similar to the previous cases, the agreement between the theoretical and simulation results is evident.

The above simulation experiments can be repeated for different cases with different step-sizes, acoustic noise signals, and secondary path models. However, in all of the cases, the theoretical model, given by Eqs. (95) and (96), can effectively describe system behaviors in the simulation. In fact, the agreement between the theoretical and simulation results takes away the ambiguity of the independence assumptions used in the derivation of the theoretical model. The verification of this model is important at this stage because this model will be used for the further investigations in this research line.

V. Conclusion

A theoretical framework for stochastic modeling of FxLMS-based ANC systems in general conditions is developed in this paper. This model considers a realistic secondary path, an stochastic acoustic noise with an arbitrary band-width,

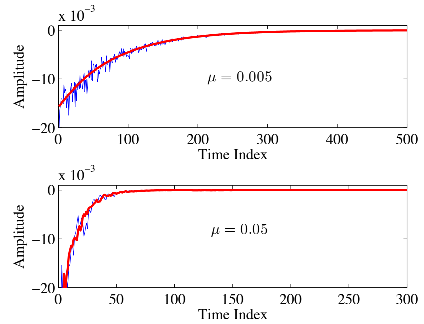

(a) Case 1

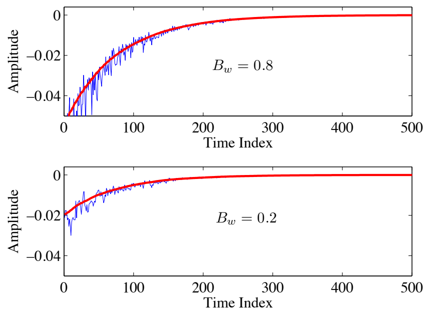

(b) Case 2

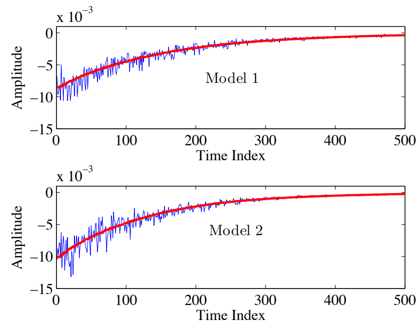

(c) Case 3

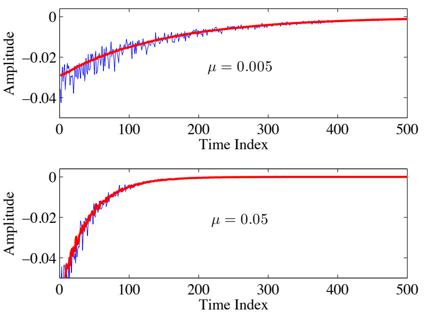

(d) Case 4

Figure 5: Variations of $\triangle J_{ex}(n)$ for different step-sizes and in different working conditions, red lines: theoretical results, blue lines: computer simulation

and an arbitrary secondary path model. This means that this comprehensive model can precisely determine behaviors of practical FxLMS-based ANC systems.

Acknowledgment

This research is supported by The University of Auckland FRDF grant; Project Number: 3700501.

References

[1] L. Resende and J. Bermudez, "Statistical analysis of the fxlms algorithm about the steady-state solution," *Telecommunications Symposium, 2006 International*, pp. 306–309, Sept. 2006.

[2] O. Tobias, J. Bermudez, and N. Bershad, "Mean weight behavior of the filtered-x lms algorithm," *Signal Processing, IEEE Transactions on*, vol. 48, no. 4, pp. 1061–1075, Apr 2000.

[3] G. Long, F. Ling, and J. Proakis, "The LMS algorithm with delayed coefficient adaptation," *Acoustics, Speech and Signal Processing, IEEE Transactions on*, vol. 37, no. 9, pp. 1397–1405, September 1989.

[4] ——, "Corrections to 'The LMS algorithm with delayed coefficient adaptation'," *Signal Processing, IEEE Transactions on*, vol. 40, no. 1, pp. 230–232, January 1992.

[5] S. J. Elliott and P. A. Nelson, "Multiple-point equalization in a room using adaptive digital filters," *Journal of the Audio Engineering Society*, vol. 37, no. 11, pp. 899–907, November 1989.

[6] E. Bjarnason, "Analysis of the filtered-x LMS algorithm," *Speech and Audio Processing, IEEE Transactions on*, vol. 3, no. 6, pp. 504–514, November 1995.

[7] I. Tabatabaei Ardekani and W. H. Abdulla, "Theoretical convergence analysis of FxLMS algorithm," *Signal Processing*, vol. 90, no. 12, pp. 3046 – 3055, 2010.

[8] ——, "On the convergence of real-time active noise control systems," *Signal Processing*, vol. 91, no. 5, pp. 1262 – 1274, 2011.

[9] ——, "On the stability of adaptation process in active noise control systems," *Journal of Acoustical Society of America*, vol. 129, no. 1, pp. 173–184, 2011.

[10] ——, "Effects of imperfect secondary path modeling on adaptive active noise control systems," *Control Systems Technology, IEEE Transactions on*, vol. PP, no. 99, pp. 1 –11, 2011 - Available Online.

[11] L. Vicente and Masgrau, "Novel FxLMS Convergence Condition With Deterministic Reference," *Signal Processing, IEEE Transactions on*, vol. 54, no. 10, pp. 3768–3774, October 2006.

[12] Y. Takenouchi, H. Sizuhi, and A. Omoto, "Behavior of the practically implemented filtered reference LMS algorithm in an active noise control system," *Journal of Acoustical science and technology*, vol. 27, pp. 20–27, 2006.

[13] Y. Xiao, A. Ikuta, L. Ma, and K. Khorasani, "Stochastic Analysis of the FXLMS-Based Narrowband Active Noise Control System," *Audio, Speech, and Language Processing, IEEE Transactions on*, vol. 16, no. 5, pp. 1000–1014, July 2008.

[14] S. M. Kuo and D. R. Morgan, *Active noise control systems: algorithms and DSP implementations*. New York, NY, USA: Wiley Interscience, 1996.

[15] B. Widrow, D. Shur, and S. Shaffer, "On adaptive inverse control," in *Proceeding of the 15th Asilomar Conference on Circuits, Systems and Computers*, November 1981, pp. 185–189.

[16] S. Haykin, *Adaptive Filter Theory*, 4th ed. Prentice Hall, 2002.

[17] W. A. Gardner, "Learning characteristics of stochastic gradient descent algorithm: A general study, analysis and critique," *Signal Processing*, vol. 6, pp. 113–133, 1984.

[18] B. Widrow and S. D. Stearns, *Adaptive Signal Processing*. Prentice Hall, 1985.

[19] A. H. Sayed, *Adaptive Filters*. Wiley Interscience, 2008.